

Southern Hemisphere jet latitude biases in CMIP5 models linked to shortwave cloud forcing

Paulo Ceppi,¹ Yen-Ting Hwang,¹ Dargan M. W. Frierson,¹ and Dennis L. Hartmann¹

Received 13 July 2012; revised 4 September 2012; accepted 4 September 2012; published 5 October 2012.

[1] Substantial biases in shortwave cloud forcing (SWCF) of up to $\pm 30 \text{ W m}^{-2}$ are found in the midlatitudes of the Southern Hemisphere in the historical simulations of 34 CMIP5 coupled general circulation models. The SWCF biases are shown to induce surface temperature anomalies localized in the midlatitudes, and are significantly correlated with the mean latitude of the eddy-driven jet, with a negative SWCF bias corresponding to an equatorward jet latitude bias. Aquaplanet model experiments are performed to demonstrate that the jet latitude biases are primarily induced by the midlatitude SWCF anomalies, such that the jet moves toward (away from) regions of enhanced (reduced) temperature gradients. The results underline the necessity of accurately representing cloud radiative forcings in state-of-the-art coupled models. **Citation:** Ceppi, P., Y.-T. Hwang, D. M. W. Frierson, and D. L. Hartmann (2012), Southern Hemisphere jet latitude biases in CMIP5 models linked to shortwave cloud forcing, *Geophys. Res. Lett.*, 39, L19708, doi:10.1029/2012GL053115.

1. Introduction

[2] The weather in midlatitudes is characterized by the existence of belts of westerly jet streams in each hemisphere, which are strongly related to the distribution of precipitation, cloudiness, and midlatitude storms [e.g., Wallace and Hobbs, 2006]. Near the jet streams are sharp local maxima of precipitation and surface wind stress, implying that small model errors in the latitudinal position of these features can lead to large local biases on either side of the maxima. In addition to directly affecting midlatitude climate, the jet streams are also linked to the large-scale circulation in the subtropics, as strong relationships exist between jet latitude and meridional extent of the Hadley cells and of the subtropical dry zones [Kang et al., 2011; Kang and Polvani, 2011]. Hence, accurate representation of the location and strength of the midlatitude jets is of crucial importance in climate modeling.

[3] Despite consistent improvements in resolution and increasing complexity of the represented processes, current state-of-the-art coupled global circulation models (CGCMs) are known to exhibit significant biases in mean jet latitude, with most models having the jet too far equatorward [e.g., Gerber et al., 2010; Barnes and Hartmann, 2010]. Such biases are known to affect a number of phenomena, includ-

ing the frequency of blocking anticyclones [Scaife et al., 2010], the distribution of surface wind stress and its impacts on ocean currents [Fyfe and Saenko, 2006], and the persistence of the annular modes [Barnes and Hartmann, 2010]. Moreover, jet latitude biases are of importance in the context of climate change, as the magnitude of the projected jet shift due to increasing greenhouse gases is directly related to the mean latitude of the jet in CGCMs [Kidston and Gerber, 2010].

[4] In this paper, we analyze Southern Hemispheric (SH) jet latitude biases in 34 CGCMs from the archive of the Coupled Model Intercomparison Project phase 5 (CMIP5) [Taylor et al., 2012]. We show that a substantial fraction of the biases in jet latitude can be explained by anomalies in midlatitude (40° – 60° S) shortwave forcing due to clouds. In particular, models with anomalously negative cloud shortwave forcing tend to exhibit an equatorward bias in jet latitude. We demonstrate that this bias is consistent with the results of aquaplanet model experiments where a radiative forcing is applied in midlatitudes. The response of the jet to the forcing can be explained mainly by changes in meridional surface temperature gradients and baroclinicity.

2. Data and Methods

[5] We examine the zonal mean climatology of historical integrations from 34 CMIP5 models, listed in Table 1. For comparison with reanalysis data sets, the data are averaged over the time period 1979 to 2005. The variables considered are zonal wind, surface air temperature, and the top of atmosphere (TOA) shortwave cloud forcing (SWCF), which is calculated as clear-sky minus all-sky outgoing TOA shortwave radiation. All results shown in this paper are for annual-mean values.

[6] The SWCF in CGCMs is compared with satellite-based TOA SWCF estimates from the Clouds and the Earth's Radiant Energy System Energy Balanced and Filled (CERES EBAF) data set, covering the time period 2000–2010 [Wielicki et al., 1996]. Although the CERES and the CGCM SWCF data are based on different time periods, we verified that the mean SWCF values are only weakly dependent on the exact time frame of consideration, making a comparison of the different data sets possible. In addition, we utilize zonally-averaged zonal wind and surface temperature data from the ERA-Interim [Dee et al., 2011] and NCEP [Kalnay et al., 1996] reanalyses, averaged over 1979–2005.

[7] We use the GFDL AM2.1 model [Delworth et al., 2006] in aquaplanet configuration with a slab ocean lower boundary and perpetual equinox conditions. In all experiments, the model is run for six years, after discarding the first two years of spin-up. To assess the effect of anomalies in midlatitude shortwave radiation, we impose an anomalous

¹Department of Atmospheric Sciences, University of Washington, Seattle, Washington, USA.

Corresponding author: P. Ceppi, Department of Atmospheric Sciences, University of Washington, Box 351640, Seattle, WA 98195-1640, USA. (ceppi@atmos.washington.edu)

Table 1. List of CMIP5 CGCMs Used in the Analysis^a

	Model Name	Institute
1	ACCESS1.0	CSIRO-BOM
2	ACCESS1.3	CSIRO-BOM
3	BCC-CSM1.1	BCC
4	BNU-ESM	GCESS
5	CanESM2	CCCMA
6	CCSM4	NCAR
7	CESM1-FASTCHEM	NSF-DOE-NCAR
8	CNRM-CM5	CNRM-CERFACS
9	CSIRO-Mk3.6.0	CSIRO-QCCCE
10	FGOALS-s2	LASG-IAP
11	FIO-ESM	FIO
12	GFDL-CM3	NOAA GFDL
13	GFDL-ESM2G	NOAA GFDL
14	GFDL-ESM2M	NOAA GFDL
15	GISS-E2-H	NASA GISS
16	GISS-E2-R	NASA GISS
17	HadCM3	MOHC
18	HadGEM2-AO	MOHC
19	HadGEM2-CC	MOHC
20	HadGEM2-ES	MOHC
21	INMCM4	INM
22	IPSL-CM5A-LR	IPSL
23	IPSL-CM5B-LR	IPSL
24	IPSL-CM5A-MR	IPSL
25	MIROC-ESM	MIROC
26	MIROC-ESM-CHEM	MIROC
27	MIROC4h	MIROC
28	MIROC5	MIROC
29	MPI-ESM-LR	MPI-M
30	MPI-ESM-MR	MPI-M
31	MPI-ESM-P	MPI-M
32	MRI-CGCM3	MRI
33	NorESM1-M	NCC
34	NorESM1-ME	NCC

^aFor all models, the first ensemble member of the historical experiment (“r1i1p1”) was analyzed over the period 1979–2005.

radiative flux at the ocean surface, calculated as

$$F = \frac{A}{\cos \phi} \exp \left[- \left(\frac{|\phi| - \phi_m}{\sigma} \right)^2 \right], \quad (1)$$

corresponding to a Gaussian function where $\sigma = 10^\circ$ and $A = \pm 30 \text{ W m}^{-2}$. ϕ_m is varied from 40° to 70°S in 10-degree increments to investigate the effect of the latitude of the imposed radiative forcing, and division by $\cos \phi$ ensures that the total energy input remains constant for forcings centered at different latitudes for a given value of A . To increase the sample size, the forcings are applied in both hemispheres, symmetrically about the Equator, and the results are averaged over both hemispheres.

[8] We define the location of the midlatitude (or eddy-driven) jet as the latitude of the maximum zonally-averaged zonal wind in the lower troposphere (850 hPa in the CGCMs, surface level in the aquaplanet model). The zonal wind distribution is cubically interpolated (using the four nearest neighbor gridpoints) at a latitudinal resolution of 0.1° prior to calculating the jet latitude.

3. Biases in CMIP5 CGCMs

[9] Observed SWCF (black line in Figure 1) has its minimum near the SH storm track where clouds in different sectors of extratropical cyclones reflect substantial shortwave radiation back to space. Differences in simulated SWCF are

considerable among CGCMs (Figure 1, top), with particularly large spread found in the SH midlatitudes and in the deep tropics, even though the multi-model mean is quite close to the CERES values. The intensity of the SH midlatitude minimum varies by up to $\pm 30 \text{ W m}^{-2}$ in the SH.

[10] Given the magnitude of the SWCF variations, it is not surprising to find large differences in mean surface temperature between CGCMs (Figure 1, bottom). To emphasize the relationship between anomalies in midlatitude SWCF and temperatures, we color-coded the models in Figure 1 by the magnitude of their SWCF peak between 40° and 60°S . This reveals that midlatitude surface temperature anomalies are dominated by the biases in SWCF ($r = 0.63$).

[11] It is worth noting that although the sign of the SWCF anomalies tends to be the same in the midlatitudes of both hemispheres for each CGCM, the relationships between SWCF, midlatitude surface temperature, and jet latitude are much weaker in the Northern Hemisphere (NH). The fact that both the mean SWCF and the SWCF biases are smaller is one possible reason, since it implies a smaller SW radiative effect due to clouds. We will focus on the SH in the remainder of this study.

[12] Numerous studies based on idealized model experiments have shown that the mean circulation, and particularly the eddy-driven jets, respond to thermal forcings [see, e.g.,

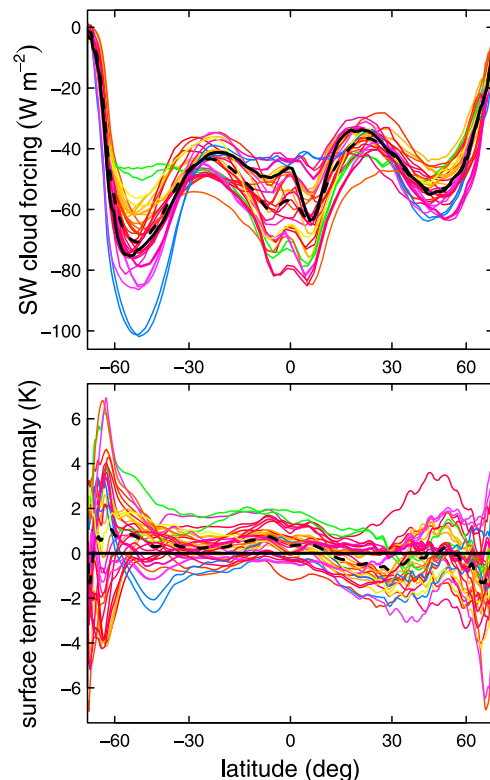


Figure 1. Mean shortwave cloud forcing (SWCF) and surface temperature anomaly as a function of latitude for each of the CGCMs. Each line is colored according to the magnitude of the respective peak SWCF between 40° and 60°S (see text), and the solid black line represents CERES data. The dashed lines correspond to the multi-model mean SWCF and temperature anomaly. The surface temperature anomalies are computed relative to NCEP values.

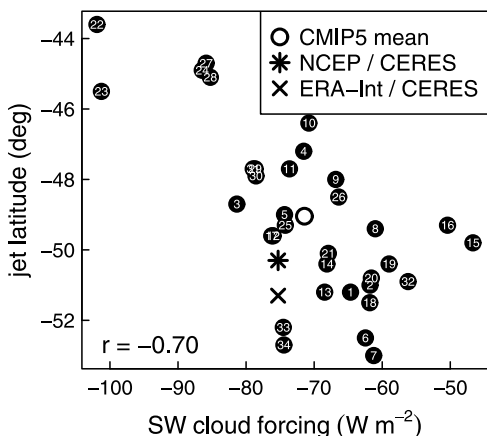


Figure 2. Mean jet latitude as a function of peak SWCF in SH midlatitudes (see Figure 1 and text). The numbers refer to the CGCMs in Table 1.

Kushner et al., 2001; Polvani and Kushner, 2002; Brayshaw et al., 2008; Chen et al., 2010; Allen et al., 2012]. Such responses may arise from several types of forcings. One example are global- or hemispheric-scale forcings, such as the effect of increasing greenhouse gas concentrations, where warming the troposphere induces a poleward shift of the eddy-driven jet [*Kushner et al., 2001*]. However, more localized forcings may also alter the distribution of eddy activity, inducing a shift of the jet toward (away from) the increased (decreased) meridional surface temperature gradient [*Brayshaw et al., 2008; Chen et al., 2010*]. Such a response can be understood from the perspective of changes in baroclinicity, since Eady growth rates are proportional to the meridional temperature gradients.

[13] Given that the biases in SWCF induce thermal anomalies, it is legitimate to ask whether they also induce shifts in jet latitude in the considered CGCMs. Figure 2 shows the latitude of the eddy-driven jet versus the magnitude of the peak SWCF in SH midlatitudes, as defined above. We find a highly significant negative correlation ($r = -0.70$; $p = 4.0 \times 10^{-6}$), such that the CGCMs with an anomalously strong midlatitude SWCF – and therefore anomalously cold midlatitudes – have an equatorward bias in jet position. The opposite tends to be true of models with anomalously weak SWCF in midlatitudes, although the relationship is somewhat less clear. Overall, SWCF biases explain about half of the variance in jet latitude ($r^2 = 49\%$).

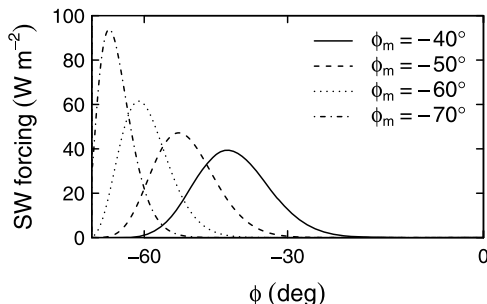


Figure 3. Shape of the applied radiative forcings as a function of ϕ_m (see equation (1)) for $A = 30 \text{ W m}^{-2}$.

Note that this relationship remains essentially unchanged if the mean midlatitude ($40^\circ\text{--}60^\circ \text{ S}$) SWCF is used instead of the peak value. In addition, the strength of the relationship is similar if individual seasons are considered instead of annual-mean values (not shown).

[14] A careful examination of Figure 2 also reveals that the negative SWCF biases are dominated by the IPSL models (numbers 22–24) and the MIROC-ESM models (27–28). Omitting these, the correlation between jet latitude and SWCF drops to -0.37 , but remains significant at the 5% level ($p = 0.03$).

[15] From the structure and magnitude of the SWCF biases in Figure 1, we infer that the biases in jet latitude are likely a result of the SWCF biases and not vice versa. We verified that interannual variations in jet latitude *within each model* induce changes in SWCF of the order of a few W m^{-2} , considerably smaller than the observed differences in SWCF *between models*. Thus, the large magnitude of the SWCF anomalies in some of the CGCMs makes it unlikely that they could merely result from changes in jet latitude caused by other forcings. We therefore expect that the SWCF biases result from errors in cloud fraction or optical depth over the entire midlatitudes, ultimately due to the cloud parameterization schemes, and that these in turn cause the jet latitude biases.

[16] It should also be noted that while the multi-model mean jet latitude (49° S) is equatorward of the reanalyses, the mean peak SWCF in SH midlatitudes is close to the CERES values (-71 W m^{-2} vs. -74 W m^{-2}), suggesting that there may be other mechanisms, in addition to SWCF biases, that cause the biases in jet latitude. Nevertheless, the strong correlation found between SWCF and jet latitude biases supports the idea that the thermal forcings induced by SWCF anomalies explain at least part of the observed spread in jet latitude.

4. Mechanisms for Cloud Influences on Jet Latitude

[17] The negative correlation between SWCF and jet latitude suggests two possible mechanisms: a positive SWCF anomaly causes a net warming of the hemisphere, and also induces a change in meridional surface temperature gradients such that the strongest gradients are shifted poleward, with both mechanisms potentially leading to a poleward shift

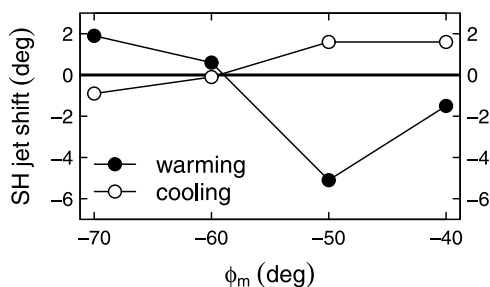


Figure 4. Response of the SH jet in the aquaplanet model experiments as a function of the latitude ϕ_m of the imposed radiative forcing, with $A = \pm 30 \text{ W m}^{-2}$. Positive values correspond to an equatorward shift. The control jet latitude is 44° S .

of the jet. To assess the relevance of each of these mechanisms, we performed aquaplanet model experiments with imposed, anomalous radiative fluxes at the ocean surface in mid to high latitudes (see Data and Methods and equation (1)). The shape of the imposed forcing with $\phi_m = 50^\circ\text{S}$ mimics the typical SWCF anomaly in the SH midlatitudes found in the CMIP5 CGCMs, and we also apply forcings confined to lower and higher latitudes. Two sets of experiments were carried out, one of which is represented in Figure 3; the other set is identical but with negative forcing. These functions make it possible to test the effect of changes in meridional sea surface temperature (SST) gradient, while keeping the total, globally-averaged forcing constant within each set of experiments. Note that although we cannot reproduce possible effects of atmospheric SW absorption with our experimental approach, we expect the effect of changes in SW absorption at the surface to be dominant, and this is the effect we seek to reproduce in our model experiments.

[18] The response of the jet to the forcings is shown in Figure 4. The magnitude of the response in the aquaplanet model is relatively small, with jet shifts of generally two degrees or less, except for the warming case at 50°S . However, we find that the jet shift is consistent with the change in meridional SST gradient induced by the forcing. When a positive radiative forcing (warming) is applied in midlatitudes, the SST gradient increases poleward of the climatological jet position and decreases equatorward of it; however, when the warming occurs in high latitudes (poleward of about 60°S), the midlatitude SST gradient decreases. In both cases, the jet moves toward (away from) the region of increased (decreased) baroclinicity, consistent with the findings of *Brayshaw et al.* [2008] and *Chen et al.* [2010]. The same reasoning can be applied to the cooling experiments.

[19] Interestingly, the strongest response is obtained when the forcing is applied at 50°S , coincident with the latitude of peak SWCF biases and with the mean jet latitude in the CGCMs. If the eddy-driven jet shifts due to localized changes in baroclinicity, then one would expect to find the strongest response for a radiative anomaly near the climatological jet latitude. In the aquaplanet model, the eddy-driven jet is situated near 44°S in the control experiment, at a lower latitude than in most CGCMs, and this may affect the magnitude of the response to the different forcings. Overall, however, the aquaplanet model results are consistent with the idea that an anomalous radiative forcing localized near the climatological jet position (i.e., in midlatitudes) induces a jet shift toward the flank of increased baroclinicity.

[20] Finally, it is also important to note that in this series of experiments, the change in SST gradients overwhelms the response due to the net global warming or cooling; for instance, in the warming cases, the mean global tropospheric temperature always increases, since there is a net input of radiative energy, but the jet does not always shift poleward. Hence, the dominant mechanism in explaining the jet response appears to be the change in meridional SST gradients induced by the localized heating or cooling in midlatitudes. This conclusion is further strengthened by the fact that the latitude of the jet in the CMIP5 CGCMs is not well-

correlated with the hemispherically-averaged mean surface temperature ($r = 0.20$; not shown).

5. Conclusions

[21] We show that the CMIP5 CGCMs exhibit large ($\pm 30 \text{ W m}^{-2}$) shortwave cloud forcing (SWCF) biases in the SH midlatitudes, and that these biases are related to substantial surface temperature anomalies in the same latitude range. At the same time, the SWCF anomalies are significantly correlated with the latitude of the SH eddy-driven jet, with negative SWCF anomalies corresponding to equatorward jet biases.

[22] We interpret our findings in terms of changes in meridional surface temperature gradients and baroclinicity. Because the SWCF-driven thermal anomalies are localized in the midlatitudes, they induce a dipole of SST gradient changes that maximize just poleward and equatorward of the climatological eddy-driven jet position. The response of the jet is consistent with a shift toward (or away from) the region of enhanced (reduced) baroclinicity, and this is confirmed by aquaplanet model experiments with anomalous radiative forcings in mid or high latitudes.

[23] The results from the present study demonstrate that despite consistent improvements in resolution and complexity, accurately representing clouds and their radiative effects remains a challenge for state-of-the-art GCMs, and further improvements in the representation of these effects will be necessary to reduce errors in the simulation of the mean atmospheric circulation. While our idealized model experiments suggest that reducing the SWCF biases would reduce jet latitude biases to some extent, this should be verified by directly altering cloud parameterizations in CGCMs. Although such experiments will likely induce other biases in the CGCMs as a side effect, we hope that the relations and mechanisms presented here will eventually aid in the reduction of biases in climate models.

[24] **Acknowledgments.** The authors thank D. J. Brayshaw and T. Reichler, whose reviews helped improve the manuscript. This work was supported by the National Science Foundation. P.C. and D.L.H. were funded by grant AGS-0960497, Y.-T.H. and D.M.W.F. by grants ATM-0846641 and ATM-0936059. The CERES data were obtained from the NASA Langley Research Center Atmospheric Science Data Center. We acknowledge the World Climate Research Programme's Working Group on Coupled Modelling, which is responsible for CMIP, and we thank the climate modeling groups (listed in Table 1 of this paper) for producing and making available their model output. For CMIP the U.S. Department of Energy's Program for Climate Model Diagnosis and Intercomparison provides coordinating support and led development of software infrastructure in partnership with the Global Organization for Earth System Science Portals.

[25] The editor thanks Thomas Reichler and David Brayshaw.

References

- Allen, R. J., S. C. Sherwood, J. R. Norris, and C. S. Zender (2012), Recent Northern Hemisphere tropical expansion primarily driven by black carbon and tropospheric ozone, *Nature*, *485*, 350–354.
- Barnes, E. A., and D. L. Hartmann (2010), Testing a theory for the effect of latitude on the persistence of eddy-driven jets using CMIP3 simulations, *Geophys. Res. Lett.*, *37*, L15801, doi:10.1029/2010GL044144.
- Brayshaw, D. J., B. Hoskins, and M. Blackburn (2008), The storm-track response to idealized SST perturbations in an aquaplanet GCM, *J. Atmos. Sci.*, *65*, 2842–2860.
- Chen, G., R. A. Plumb, and J. Lu (2010), Sensitivities of zonal mean atmospheric circulation to SST warming in an aqua-planet model, *Geophys. Res. Lett.*, *37*, L12701, doi:10.1029/2010GL043473.

- Dee, D. P., et al. (2011), The ERA-Interim reanalysis: Configuration and performance of the data assimilation system, *Q. J. R. Meteorol. Soc.*, *137*, 553–597.
- Delworth, T. L., et al. (2006), GFDL’s CM2 global coupled climate models. Part I: Formulation and simulation characteristics, *J. Clim.*, *19*, 643–674.
- Fyfe, J. C., and O. A. Saenko (2006), Simulated changes in the extratropical Southern Hemisphere winds and currents, *Geophys. Res. Lett.*, *33*, L06701, doi:10.1029/2005GL025332.
- Gerber, E. P., et al. (2010), Stratosphere-troposphere coupling and annular mode variability in chemistry-climate models, *J. Geophys. Res.*, *115*, D00M06, doi:10.1029/2009JD013770. [Printed 116(D3), 2011.]
- Kalnay, E., et al. (1996), The NCEP/NCAR 40-year reanalysis project, *Bull. Am. Meteorol. Soc.*, *77*, 437–471.
- Kang, S. M., and L. M. Polvani (2011), The interannual relationship between the latitude of the eddy-driven jet and the edge of the Hadley cell, *J. Clim.*, *24*, 563–568.
- Kang, S. M., L. M. Polvani, J. C. Fyfe, and M. Sigmond (2011), Impact of polar ozone depletion on subtropical precipitation, *Science*, *332*, 951–954.
- Kidston, J., and E. P. Gerber (2010), Intermodel variability of the poleward shift of the austral jet stream in the CMIP3 integrations linked to biases in 20th century climatology, *Geophys. Res. Lett.*, *37*, L09708, doi:10.1029/2010GL042873.
- Kushner, P. J., I. M. Held, and T. L. Delworth (2001), Southern Hemisphere atmospheric circulation response to global warming, *J. Clim.*, *14*, 2238–2249.
- Polvani, L. M., and P. J. Kushner (2002), Tropospheric response to stratospheric perturbations in a relatively simple general circulation model, *Geophys. Res. Lett.*, *29*(7), 1114, doi:10.1029/2001GL014284.
- Scaife, A. A., T. Woollings, J. Knight, G. Martin, and T. Hinton (2010), Atmospheric blocking and mean biases in climate models, *J. Clim.*, *23*, 6143–6152.
- Taylor, K. E., R. J. Stouffer, and G. A. Meehl (2012), An overview of CMIP5 and the experiment design, *Bull. Am. Meteorol. Soc.*, *93*, 485–498.
- Wallace, J. M., and P. V. Hobbs (2006), *Atmospheric Science: An Introductory Survey*, Academic, New York.
- Wielicki, B. A., B. R. Barkstrom, E. F. Harrison, R. B. Lee, G. Louis Smith, and J. E. Cooper (1996), Clouds and the Earth’s Radiant Energy System (CERES): An Earth observing system experiment, *Bull. Am. Meteorol. Soc.*, *77*, 853–868.